# Digital Image Correlation for Determination of Weld and Base Metal Constitutive Behavior

*A new method to determine the constitutive behavior for all of the materials comprising a weld is described*

BY A. P. REYNOLDS AND F. DUVALL

ABSTRACT. To understand and accurately model the mechanical response of welds, it is critical to have constitutive data for the various microstructural regions that make up the weld, *e.g.*, the fusion zone (or dynamically recrystallized zone, DRZ, in friction stir welding), the heat-affected zone (HAZ) and the base metal. Methods currently used for determining the mechanical response of the regions that constitute the weld include testing of miniature specimens excised from the weld region (Refs. 1, 2), instrumented ball indentation testing (Refs. 3, 4) and testing of bulk material produced by weld thermal simulation (Ref. 2). Each method has its advantages and disadvantages. This article describes a new method for obtaining a substantial amount of the data required to determine the constitutive behavior for all of the materials comprising a weld by performing one tensile test of a transversely loaded weld.

## Background

The new method of constitutive property determination described and demonstrated in this article makes use of an optical, full-field displacement measurement technique with good spatial resolution to determine the strain response of the weld metal, HAZ and base metal as functions of a global, remotely applied tensile loading transverse to the weld interface. The technique, based on digital image correlation (DIC), has been successfully used to measure strain fields in homogeneous materials subjected to uniform stress fields (such as tensile bars) or gradient stress fields (as at a crack tip).This article demonstrates the application of DIC to the measurement of strain fields in the heterogeneous material that comprises a friction stir weld. Because full field displacements are measured, gradients in material properties are readily observed and quantified; however, when gradients in strength are steep, there are limitations on the accuracy of the technique, as described in a separate section of the paper. One additional disadvantage of the technique is that the far-field loading is limited by the strength of the weakest component of the weld microstructure: the weld is treated as a composite material undergoing a nominally iso-stress loading condition. Therefore, the strain range over which the constitutive behavior of a particular region of the weld is measured will be inversely dependent on the strength of that region.

Compared to the new method of constitutive property determination, testing of miniature samples from each region of the weld allows determination of constitutive properties from yield to fracture. However, there are difficulties associated with production and testing of the miniature specimens required, and if steep gradients in material properties exist within the weldment, then even a very small specimen may not exhibit homogeneous properties. In addition to the precise and careful machining techniques required to produce the sub-miniature specimens, the capability of performing accurate mechanical tests on such specimens is not generally available.

Ball indentation testing may be performed semi-nondestructively and in the field. The technique has good spatial resolution; however, determination of important constitutive data, such as the yield strength, requires curve fitting of flow stress data from high strain levels (>0.04) and a priori knowledge of empirically derived material constants (Ref. 3).

Use of bulk material from weld thermal simulation allows testing of full-size tensile specimens and determination of properties from yield to fracture; however, the highly transient thermal histories experienced by welded joints are difficult to characterize accurately and to reproduce (Ref. 2).

KEY WORDS

Digital Image Correlation
Friction Stir Welding
Fusion Zone
Heat-Affected Zone
Stress-Strain Response
Tensile Test
Weld Nugget

*A. P. REYNOLDS and F. DUVALL are with the Department of Mechanical Engineering, University of South Carolina, Columbia, S.C.*

### Full Field Displacement Measurement with Digital Image Correlation

The use of DIC for determination of surface displacement and strain fields in homogeneous materials has been discussed in great detail in previous papers; however, a brief discussion of the technique will be presented here (Refs. 5–7). Digital image correlation is a method by which the relative displacement of image features from one image to another can be determined automatically. If numerous points in an image are "correlated," a displacement field for the image can be produced. In this work, we illustrate the use of DIC to produce displacement fields for images of the transversely loaded weld specimens corresponding to different global stress levels. By suitable postprocessing, the displacement fields are converted to strain fields.

To obtain correlatable images, a high-contrast pattern must be applied to the surface to be imaged (in this case, the tensile bar). A white spray-painted back-

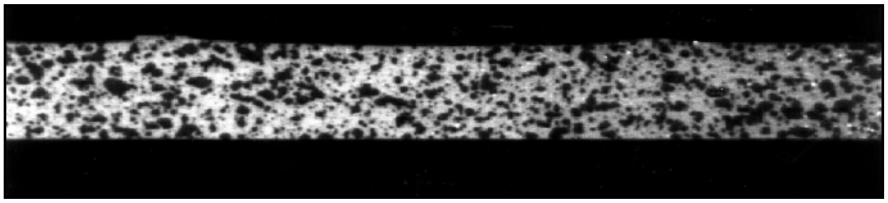

*Fig. 1 — Typical high-contrast pattern used for digital image correlation as applied to a transverse weld tensile specimen.*

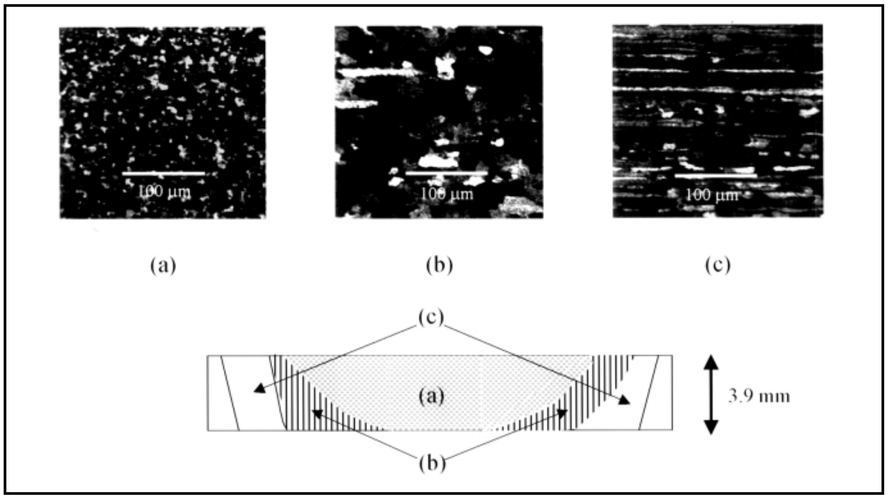


*Fig. 2 — Schematic drawing of a friction stir weld cross section and micrographs of: A — The dynamically recrystallized zone in the weld nugget; B — recrystallized base metal; C — recovered and partially recrystallized base metal.*

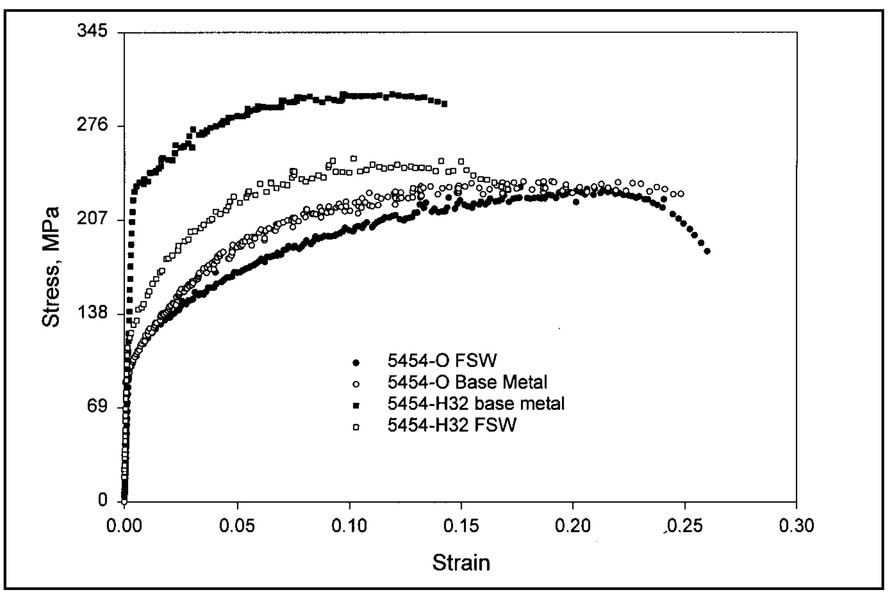


*Fig. 3 — Tensile stress-strain curves for 5454-O base metal, 5454-H32 base metal and transverse FSW in 5454-O and 5454-H32.*

ground with a black overspray provides the necessary contrast in the images. A black-and-white, 8-bit digital camera with a 768 X 484 pixel sensor array is used to acquire the images through a 200-mm telephoto lens. The optimum scale of the pattern depends on the spatial resolution desired and, hence, the magnification that is used to view the pattern. An example of a typical pattern used in this work is shown in Fig. 1 applied to the through-thickness plane of a transverse friction stir weld tensile bar.

Once the tensile specimen, with pattern applied, has been loaded into the tensile testing machine, an initial image of the undeformed specimen is acquired. Subsequent images are acquired at specified intervals of applied load or overall specimen strain (deformed images). Each of the deformed images is correlated with the initial undeformed image to determine the displacement of image subsets between the two images. The displacement measured between any two pairs of images is always displacement relative to the initial undeformed state. The subset displacements are used to generate a displacement field that is subsequently smoothed.

After the smoothed displacement fields are obtained, the data are processed to obtain strain data. Two methods have been used to determine strain from the displacement data in this study. The simplest method used is to fit a polynomial function to the displacement, u, in the loading direction, x. The first derivative, $\partial u/\partial x$, of the fit function is determined at all the points of interest (corresponding to particular locations relative to the weld centerline). This derivative is the strain at the chosen locations. A more complex scheme is to fit a surface to the u and v displacements. The displacement gradients on the surface correspond to the strains in any chosen direction. Using this technique, principal strains, shear strains and longitudinal and transverse strains can be obtained. The strain determined by either technique is plotted against corresponding levels of global stress and, thus, assuming the validity of the isostress assumption, stress-strain curves are created for any chosen region of the weld, HAZ and/or base metal. If it is desired, data may be obtained for the specimen position corresponding to each pixel in the original, undeformed image. The maximum strain that can be measured via the DIC technique is limited mainly by breakdown of the high-contrast pattern applied to the specimen. In the authors' experiments, strain levels to 25% have been measured.

## Materials and Experimental Procedure

### Base Metal Microstructure

The materials used for this study were 3.9-mm-thick sheets of 5454-O and 5454-H32 aluminum alloys. Alloy 5454 is a solid-solution-strengthened, strain-hardenable aluminum alloy with a nominal composition (wt-%) of 2.7Mg-0.8Mn-0.12Cr-balance aluminum. Metallographic specimens were prepared by mechanical polishing and elec-

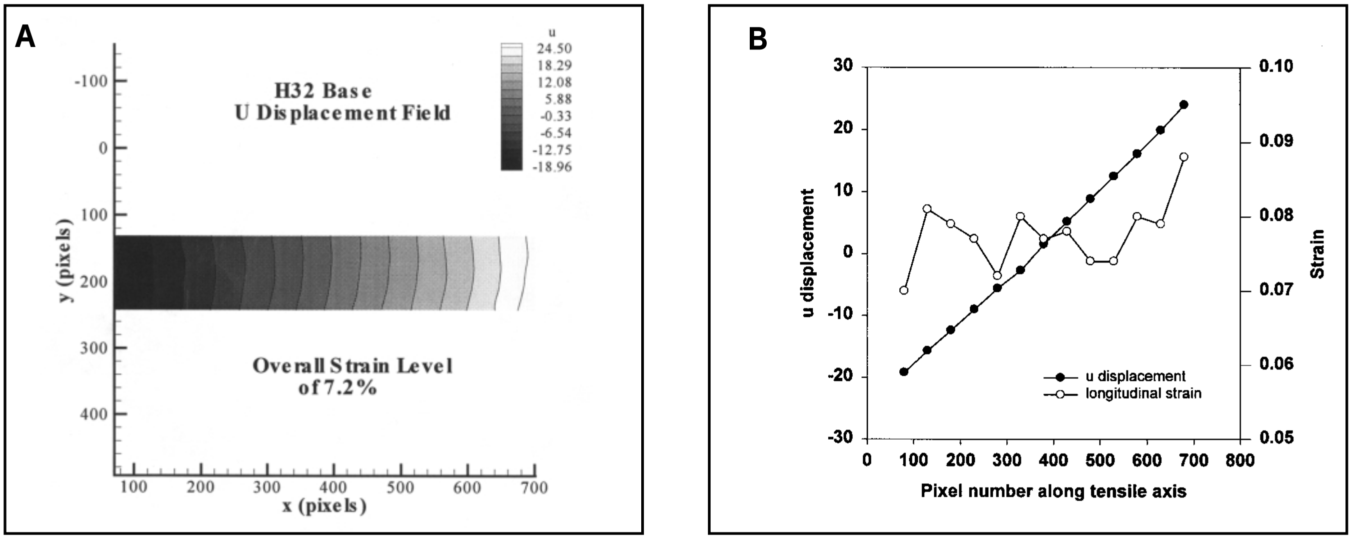


*Fig. 4 — A — Contour plot showing the raw, DIC-derived u-displacement data for a 5454-H32 base metal tensile specimen at an overall strain of 7.2%; B — specimen centerline u-displacement and corresponding longitudinal strain as a function of position along loading direction.*

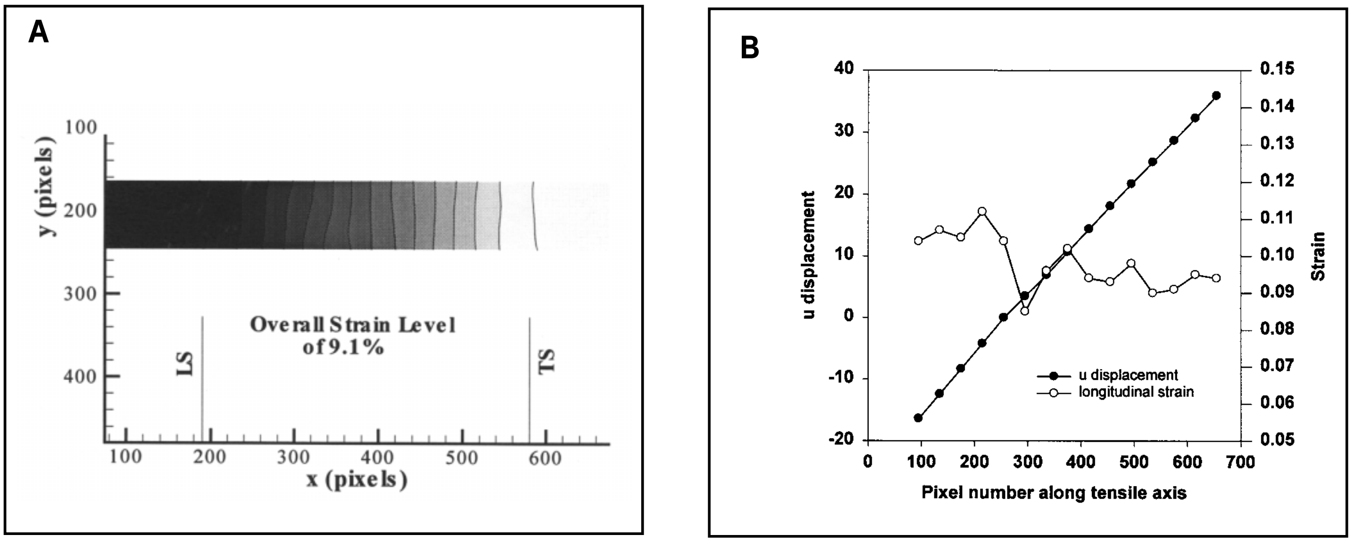


*Fig. 5 — A — Contour plot showing the raw, DIC-derived u-displacement data for a transverse FSW in 5454-O at an overall strain of 9.3%; B — specimen centerline u-displacement and corresponding longitudinal strain as a function of position along loading direction.*

trolytic etching in Barker's reagent. The O-temper material was fully recrystallized with nearly equiaxed grains. A mean-linear-intercept grain size of 40 micrometers was determined for this material. The H32 temper material was cold rolled and unrecrystallized with grains that were highly elongated in the direction of rolling.

### Friction Stir Welding of 5454

An autogenous friction stir weld was made between two 70 X 610-mm sheets of 3.9-mm-thick 5454-H32. The weld was made on a vertical milling machine using a typical friction stir welding tool. The shoulder diameter of the tool was 18 mm and the pin diameter 4.5 mm. The length of the pin was slightly less than the sheet thickness. For the welds under consideration here, the spindle speed was 270 rpm and the welding rate (traverse speed) was 1.4 mm $s^{-1}$ (3.4 in./min). The tool was tilted 3 deg from normal to the work. The workpieces were held down by steel angles clamped every 6 in. to prevent bulging of the work ahead of the advancing welding tool. The clamping angles were approximately 22 mm from the centerline of the weld.

### Mechanical Testing Procedures

All tensile tests were performed on a 100-kN (22-kip) servohydraulic test machine operated in ram-displacement control. Standard subsize tensile bars (gauge length = 50.8 mm), machined from the 3.9-mm-thick 5454-O and 5454-H32 base metal, were tested at ambient temperature and at a nominal, initial strain rate of 1 X $10^{-3}s^{-1}$ (Ref. 8). Specimen strain was monitored with a 25.4-mm (1-in.) gauge length extensometer.

Friction stir welds were tensile tested in the transverse orientation (welding direction perpendicular to loading direction). Digital image correlation was used to measure local strain in the H32 base metal, in a transversely loaded O-temper friction stir weld and in an H32 friction stir weld.

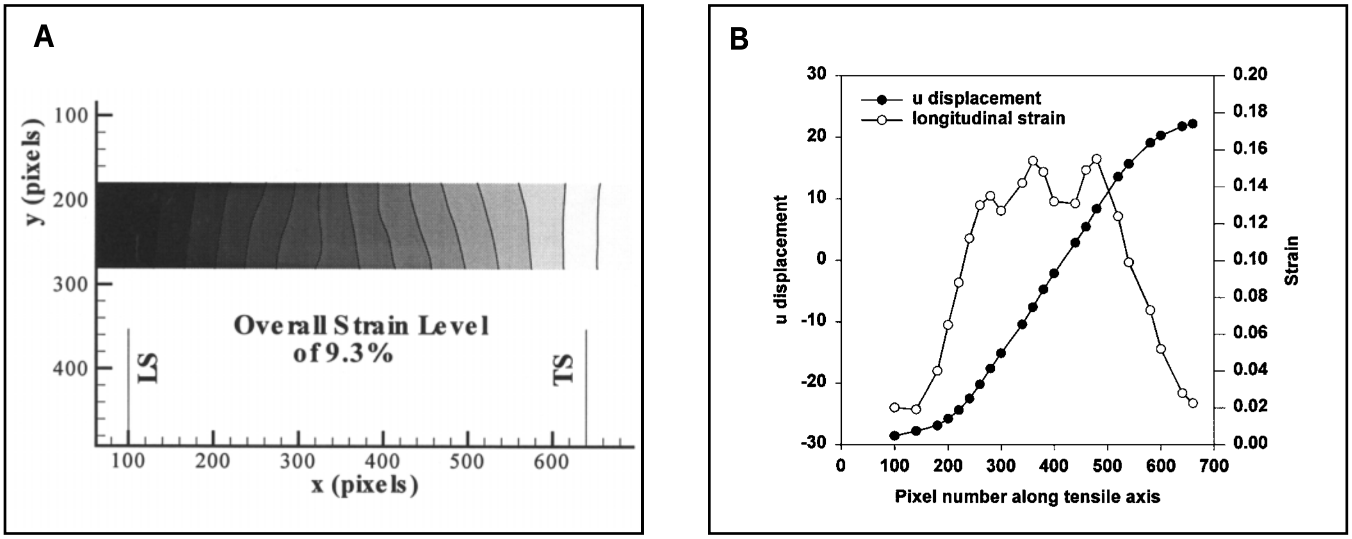


*Fig. 6 — A — Contour plot showing the raw, DIC-derived u-displacement data for a transverse FSW in 5454-H32 at an overall strain of 9.1%; B — specimen centerline u-displacement and corresponding longitudinal strain as a function of position along loading direction.*

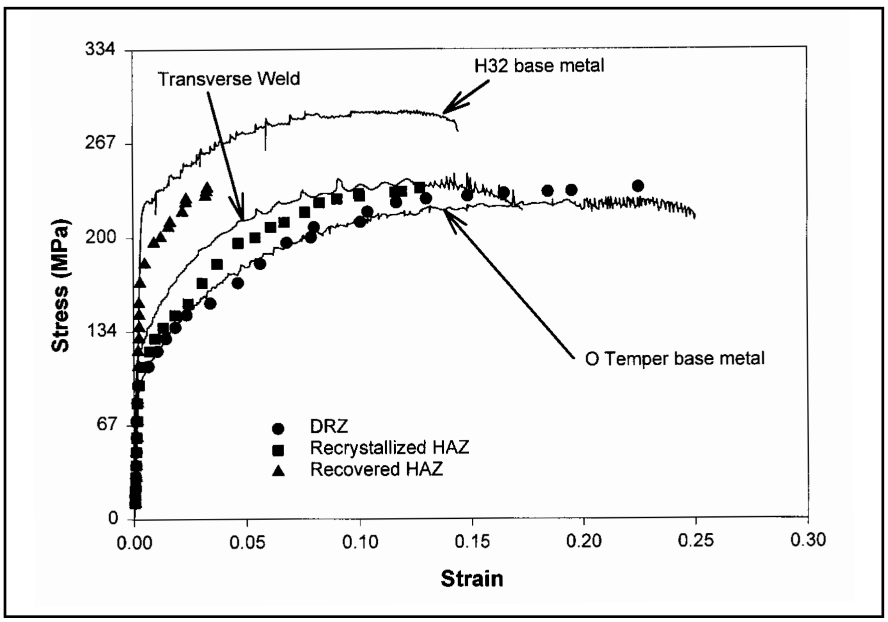


*Fig. 7 — Base metal (5454-H32 and 5454-O) and transverse weld (5454-H32) stress-strain curves with stress-strain data from specific microstructural regions determined via DIC.*

## Results and Discussion

### Weld Microstructure

Figure 2 is a schematic drawing depicting the general structure resulting from the friction stir welding process. The leading side of the weld (left in the figure) is defined as the side on which the welding tool's rotational and translational velocity vectors are of the same sign; the other side of the weld is designated the trailing side. The microstructural zones that exist in a 5454-H32 weld include (A) the DRZ, which is the region in the center of the weld dynamically recrystallized by the combined heating and plastic deformation imposed by the welding tool; (B) the recrystallized base material adjacent to but outside of the DRZ; and (C) a recovered and partially recrystallized base material region. The grain size in the DRZ is variable, but typically less than 15 micrometers, as determined by the mean linear intercept method. In the recrystallized base metal region, the grain size is variable but significantly larger than that observed in the DRZ. The extent of the heat-affected zone varies with the chosen values of the welding parameters (tool rpm and traverse rate). In a 5454-O weld, there is a dynamically recrystallized zone in the weld nugget that exhibits equiaxed grains smaller than those in the base metal. However, because the base metal is annealed and fully recrystallized, no statically recrystallized or recovered regions are observed.

### Tensile Properties

Figure 3 is a graph of the engineering stress-strain behavior of 5454-H32 base metal, 5454-O base metal, a transversely loaded 5454-O friction stir weld and a transversely loaded 5454-H32 friction stir weld specimen. The stress-strain plot for the 5454-H32 weld specimen is bracketed by the stress-strain properties of the 5454-O material and 5454-H32 base metal properties. The stress-strain behavior of the 5454-O friction stir weld specimen is nearly identical to that of the O-temper base metal.

To understand the behavior illustrated in Fig. 3, the DIC technique was used to measure local strains in and around friction stir welds in the H32 and O-temper materials. In addition, DIC was used to measure the local strain as a function of position in an H32 base metal tensile specimen that was presumed to exhibit a homogeneous response. Representative DIC data are shown in Figs. 4–6.

Figure 4 illustrates the application of DIC to the H32 base metal specimen. Figure 4A is a contour plot of the u-displacement field at an overall specimen strain of 7.2% as measured with an extensometer. The displacement, u, is in the loading direction. The displacement contours are spaced evenly, indicating uniform strain at this overall strain level. Figure 4B is a graph of the u-displacement at the specimen midplane as a function of the position along the loading axis (the solid circles) and the strain at these same positions (the open circles). The solid circles describe a relatively straight line: The strain at each position is determined from the local derivative, $\partial u/\partial x$, of the displacement data. The strains so determined vary somewhat about the overall strain level, between about 7 and 8.8%. A line fit to the entire data set gives the overall strain level of 7.2%.

Figure 5 is the same as Fig. 4 except the data are from DIC analysis of a transversely loaded friction stir weld in O-temper material. The lines marked LS and TS on the contour plot indicate the outer edges of the welding tool shoulder on the leading and trailing sides, respectively (18-mm diameter). Like the data for the H32 base metal specimen, the contours are evenly spaced, particularly at the midthickness of the weld. As for Fig. 4B, the filled circles in Fig. 5B, representing the u displacement at the midthickness, are in a nearly straight line and the strain varies from approximately 11.3 to 8.6% at an overall strain level of 9.3%. A line fit to all of the data gives an overall strain of 9.2%. Evidently, the friction stir weld in the O-temper material does not introduce a significant inhomogeneity.

Figure 6 shows data for the friction stir weld in the 5454-H32 material. Unlike the H32 base metal and the O-temper friction stir weld, the displacement contours are not evenly spaced. This can be seen on the contour plot and, in particular, on the scatter plot where it is seen the solid circles (u-displacement data) describe a sigmoidal curve. The strain in the region in and near the weld varies from approximately 2% outside the shoulder diameter to near 16% in the nugget center. The overall specimen strain corresponding to the data set shown is about 9%. In the H32 specimen, the weld does create a strong inhomogeneity in material properties, and the bulk of the plastic deformation is concentrated in the weld region where the initially strain-hardened material has been recrystallized or recovered.

Stress-strain curves for the distinct, microstructural regions in the H32 friction stir weld were assembled from multiple data sets of the type shown in Figs. 4–6 and the corresponding global stress levels. Because of the way in which the image correlation is performed, a particular location in pixel space always corresponds to a spot on the initially undeformed image and, hence, a particular position on the specimen. Stress-strain curves were determined for points on the midplane of the weld with respect to the thickness direction of the sheet at x-pixel positions of 350, 225 and 175. These pixel positions correspond respectively to points in the weld nugget center, recrystallized heat-affected zone (HAZ) and recovered HAZ.

In Fig. 7, the 5454-H32 and 5454-O base metal stress-strain curves are replotted as solid lines. The stress-strain data for the dynamically recrystallized zone (DRZ) are plotted as solid circles, the recrystallized HAZ data are plotted as solid squares and the recovered HAZ data are plotted as solid triangles. It is apparent that all of the weld-constituent tensile properties are bracketed by the properties of the strain-hardened and fully annealed base metals. The stress-strain curve of the DRZ (nugget center) tracks almost exactly the lower bound provided by the 5454-O stress-strain behavior. The H32 material, which was partially recrystallized in situ during the welding process, has a slightly elevated stress-strain response relative to the O-temper base metal. The recovered base metal is intermediate between the annealed and strain-hardened base metals in strength. These findings are not surprising, but they tend to support the accuracy of the DIC method and the assumption of iso-stress loading for determination of the constitutive properties of the weld microstructures.

Table 1 lists the 0.2% offset yield strength (YS), ultimate tensile strength (UTS) and strain-hardening exponents for the 5454-O temper, 5454-H32, the transverse weld specimen and each of the weld constituents. The weld constituent parameters were determined from the DIC-derived stress-strain curves. The numbers in the table are the inputs that might be used to define the constitutive behavior of materials for numerical modeling of the weld response. The strain-hardening exponents were determined by plotting the natural logarithm of the true stress vs. the natural logarithm of the true plastic strain between strains of 0.002 and 0.02 (chosen because the total strain in the recovered base metal was small). The slope of a straight line fit to the logarithmic data is the strain-hardening exponent. The parameters derived from the stress-strain curves for the weld constituents are again bracketed (approximately) by the O-temper and H32 constitutive behavior; the values derived from the DIC-based stress-strain curves are all reasonable based on the base metal properties and the observed behavior of the weld.

**Table 1 — Tensile Properties of Base Metals, Transverse Weld and Weld Constituents**

| | n (strain-hardening exponent) | TYS (MPa) | UTS (MPa) |
|---|---|---|---|
| 5454-O | 0.23 | 106 | 235 |
| 5454-H32 | 0.09 | 230 | 306 |
| Overall transverse weld | 0.21 | 124 | 257 |
| Recovered base | 0.14 | 186 | 244[(a)] |
| Recrystallized base | 0.21 | 109 | 244[(a)] |
| Nugget | 0.24 | 103 | 244[(a)] |

(a) Maximum stress level at which DIC data were obtained.

At first glance, it seems inconsistent that yielding should be observed in the DRZ and recrystallized base metal at stress levels of 10–15 MPa below the overall transverse weld specimen yield strength. However, the DRZ and recrystallized base metal comprise only a small part of the overall transverse weld specimen gauge length. Thus, by the time a 0.2% plastic offset is reached in the transverse weld specimen, as determined by an extensometer with a 25.4-mm gauge, the early yielding constituents have experienced significant strain hardening.

#### Factors That May Adversely Influence Accuracy of the Approach Presented

While the 5454-H32 friction stir weld has been treated as a composite material deforming under iso-stress conditions, there is the possibility of interaction between the various microstructural constituents. This interaction may mask the true constitutive properties of some of the material. Such an interaction could occur if material (*e.g.*, the weld nugget) adjacent to harder material would have its deformation constrained by the harder material in the same way that material in a notch may exhibit elevated yield strength due to the development of a triaxial stress state (Ref. 9). In essence, the material inhomogeneity will act like a geometric discontinuity. This effect may be especially pronounced in regions of steep property gradient (hence, strain gradient). However, the effect should not be noticeable at all until after yielding and after some significant plastic deformation has occurred. The effect should be less in a weld such as the one in question because the width of the softened region is significantly greater than the thickness of the sheet. In addition, the presence of the soft material should not significantly affect the deformation of the adjacent hard material. The overall effect of the property gradients present in these welds should be to slightly increase the apparent strain-hardening rates of the softer constituents in regions of the weld where they are adjacent to hard constituents. In later work, we will attempt to elucidate the effect of the property/strain gradients on the stress state in the transverse weld tensile bars via numerical analysis.

## Summary and Conclusions

The constitutive behaviors of the weld regions determined via DIC are shown to be quite reasonable when compared to the behavior exhibited by the H32 and O-temper base metals. Based on the constitutive behavior, the stress-strain response of the transverse weld specimen may be explained by assuming the weld is a composite material deforming under an iso-stress condition. It is apparent that strain initially localizes in the soft weld nugget; and as the nugget strain hardens, yield occurs at progressively greater distances from the nugget. However, minimal plastic deformation occurs in base metal that retains its original yield strength level because the ultimate tensile strength of the weld is only slightly greater than the H32 yield strength. Although the ductility of the nugget is equivalent to or greater than that of the 5454-O, the uniform elongation of the transverse weld specimen is low relative to 5454-O base metal because strain localization occurs almost immediately in the soft constituents of the weld. As expected, for a composite material loaded in an iso-stress configuration, the overall behavior is dominated by that of the weakest component of the composite. In the case of the 5454-H32 friction stir weld, that component is the weld nugget. Ultimately, it has been shown that, if the property gradients in a weld are not too steep, then the constitutive properties of the microstructural regions within a weld can be deduced from a single tensile test coupled with the DIC full-field-displacement technique. The primary advantages of the DIC-based technique compared to other methods of constitutive behavior determination in welds include the following:

1) Behavior may be determined for any or all points in the weld region with a spatial resolution limited only by the usable magnification of the imaging system and the ability to apply a pattern of appropriate scale.

2) No uncertainty exists regarding whether the material tested is actually representative of the material in the weld: The tested material is the weld material (contrast to weld simulation technique).

3) No a priori knowledge of material properties is required (*e.g.*, as in automated ball indentation tests).

*Acknowledgments*

This work was supported by an NSF-EPSCoR cooperative agreement #EPS-9630167. F. Duvall received support from the U.S. Navy during the performance of this research.

*References*

1. Zuniga, S. M., and Sheppard, S. D. 1995. Determining the constitutive properties of the heat-affected zone in a resistance spot weld. *Modelling and Simulation in Materials Science and Engineering* 3(3): 391–416.

2. Hval, M., Thaulow, C., Lange, J. H., Hoydal, S. H., and Zhang, Z. L. 1998. Numerical modeling of ductile fracture behavior in aluminum weldments. *Welding Journal* 77(5): 208-s to 217-s.

3. Haggag, F. M. 1993. *In-Situ Measurements of Mechanical Properties Using a Novel Automated Ball Indentation System*, ASTM STP 1204, eds. Corwin, Haggag and Server. ASTM, Philadelphia, Pa., pp. 27–44.

4. Haggag, F. M., Nanstad, R. K., Hutton, J. T., Thomas, D. L., and Swain, R. L. 1990. *Use of Automated Ball Indentation Testing to Measure Flow Properties and Estimate Fracture Toughness in Metallic Materials*, ASTM STP 1092, eds. Braun, Ashbaugh and Smith. ASTM, Philadelphia, Pa., pp. 188–208.

5. Wolters, W. J., Sutton, M. A., Peters, W. H., Ranson, W. F., and McNeill, S. R. 1983. Determination of displacements using an improved digital correlation method. *Computer Vision* 8: 133–139.

6. Bruck, H. A., McNeill, S. R., Sutton, M. A., and Peters, W. H., III. 1989. Digital image correlation using Newton-Raphson method of partial differential correction. *Experimental Mechanics* 29: 261–267.

7. Babai, M., Jang, J., McNeill, S. R., and Sutton, M. A. 1988. Effects of subpixel image restoration on digital correlation error estimates. *Optical Engineering* 27(10): 870–877.

8. ASTM Standard E 8-90a, *1991 Annual Book of ASTM Standards, Vol. 3.01, Metals Test Methods and Analytical Procedures*. ASTM, Philadelphia, Pa.

9. Hertzberg, R. W. 1996. *Deformation and Fracture Mechanics of Engineering Materials*, 4th ed. John Wiley and Sons, New York, N. Y., p. 51.